

Normal-Superfluid Interface Scattering For Polarized Fermion Gases

Bert Van Schaeybroeck and Achilleas Lazarides

Laboratorium voor Vaste-Stoffysica en Magnetisme,
Celestijnenlaan 200 D, Katholieke Universiteit Leuven, B-3001 Leuven, Belgium.

(Dated: March 23, 2022)

We argue that, for the recent experiments with imbalanced fermion gases, a temperature difference may occur between the normal (N) and the gapped superfluid (SF) phase. Using the mean-field formalism, we study particle scattering off the N-SF interface from the deep BCS to the unitary regime. We show that the thermal conductivity across the interface drops exponentially fast with increasing $h = k_B T$, where h is the chemical potential imbalance. This implies a blocking of thermal equilibration between the N and the SF phase. We also provide a possible mechanism for the creation of gap oscillations (FFLO-like states) as seen in recent studies on these systems.

PACS numbers: 03.75.Ss, 03.75.Hh

Introduction — An electron approaching a normal-superconducting (N-SC) interface from the normal side with energy $E < \Delta$, where Δ is the superconducting gap, has insufficient energy to excite quasiparticles inside the SC and is therefore reflected. In a SC, the relation E_F (where E_F is the Fermi energy) constrains the momentum transfer during interfacial scattering to be much lower than $2\sim k_F$, required for normal (specular) reflection. Consequently, Andreev reflection occurs: the electron pairs with another electron of opposite momentum, forming a Cooper pair. A “reflected” hole is left on the N side, which follows the time-reversed path of the incident electron. Andreev used this process to describe the unusual heat conductivity found in N-SC junctions and in the intermediate state of superconductors [1]. To date, the transport properties of such structures remain the subject of intense research [2, 3]. On the other hand, recent experiments [4, 5] have probed superfluidity in ultracold fermionic mixtures, where the possibility arises of having different chemical potentials for each species and controllable interspecies interactions. An accurate theoretical prediction of the observed density profiles is still not available, despite intense theoretical activity [6, 7, 8, 9, 10, 11, 12]. Whereas the incorporation of a normal-superfluid (N-SF) interface tension may settle this question [6, 7] for the Rice experiments, the interpretation of the MIT experiments remains unclear. A recently proposed theory [6] appears to explain all observed features, although the temperatures required for agreement with data from the MIT experiments are five times higher than observed.

In the following, we argue that the presence of a N-SF interface is likely to block thermal equilibration for these experiments, possibly inducing a temperature difference between the two phases. Incorporating such a temperature difference in the existing models may provide the key to a complete understanding of the experiments.

In this Letter we focus on two questions, to wit: 1) What are the possible reflection and transmission mechanisms at a N-SF interface? The main features distinguishing this system from a SC are the difference in the chemical potentials

and the variation of the gap from Δ to E_F as one tunes the interactions from deep BCS to the unitary regime. 2) What is the relevance of these findings for recent experimental and theoretical works?

We find a rich variety of interfacial scattering processes, depending on the energy and perpendicular momentum of the incoming particle. The scattering of the particles off the interface results in a striking decrease in the thermal conductivity for temperatures $T \sim 0.05 T_F$ (at unitarity). We also argue that upon Andreev reflection, particles and holes interfere so as to cause gap oscillations near the interface, which are observed in recent numerical studies [12]. We postpone the description of calculational details and the case of unequal fermion masses [13].

The system under study consists of two fermionic species a and b with equal masses m and chemical potentials μ_i for $i = a, b$, trapped by a potential $V(\mathbf{r})$; this gives rise to an effective chemical potential $\mu_i(\mathbf{r}) = \mu_i - V(\mathbf{r})$ (henceforth denoted by μ_i). The Bogoliubov-de Gennes (BdG) or Blonder-Tinkham-Klapwijk equations [3, 14] give a satisfactory description of this system. Denoting the particle-like and hole-like eigenfunctions of species $i = a, b$ by $u_{i,jk}$ and $v_{i,jk}$ respectively and following the standard procedure, one finds:

$$\begin{pmatrix} H_a & 0 \\ 0 & H_b \end{pmatrix} \begin{pmatrix} u_{a,jk} \\ v_{b,jk} \end{pmatrix} = E_{jk} \begin{pmatrix} u_{a,jk} \\ v_{b,jk} \end{pmatrix}; \quad (1)$$

with $H_{a,b} = \frac{\mathbf{r}^2}{2m} + \mu_{a,b} - \Delta$ where $\Delta = (\mu_a + \mu_b)/2 > 0$, $h = (\mu_a - \mu_b)/2 > 0$ and we set $\hbar = k_B = 1$. One obtains the second set of BdG Eqs. by interchanging a and b . As seen from Eqn. (1), incoming a -particles are coupled to b -holes and vice versa. Now, the prerequisite for an interface to be present between a SF with symmetrical a and b densities and an asymmetrical N phase is the existence of a first-order transition between the two phases. In the experiments, if a SF is found at the trap center, decreases upon approaching the trap boundary and probes the $(\mu_a; \mu_b)$ phase diagram, possibly inducing a crossing of the N-SF phase boundary. This happens when locally

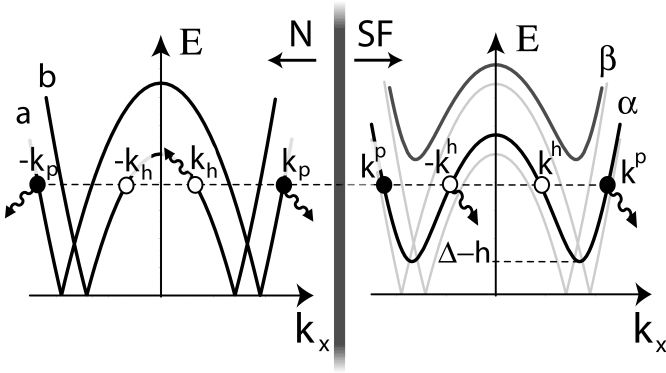


FIG. 1: The N-SF interface (thick vertical line) with the $a; b$ spectra on the N side and the gapped $\alpha; \beta$ spectra in the SF. The long dashed line cuts the spectra at particle-like (filled dots) and hole-like (empty dots) quasiparticle states, all having the same energy. An incoming a -particle (curly arrow) with momentum k_p and energy $E > \hbar$ has up to four scattering channels: the Andreev reflected k_h hole, the specularly reflected k_p particle and the transmitted hole-like k^h and particle-like k^p states.

there occurs a balance between the energy gained by creating, on the one hand, a gap and on the other hand, a density difference [17]. At $T = 0$, this local coexistence condition is well-approximated by the Clogston limit [13]:

$$\mu = \frac{p}{2} \hbar \quad (2)$$

For fixed interaction parameter $k_F a$, where a is the scattering length, the first-order transition persists at finite temperature up to a tricritical point [6, 11]. The Rice experiments are indeed accurately described using a theory incorporating a first-order transition [5, 6, 7, 8]; the MIT results are also suggestive of a first-order transition.

To model the N-SF interface, it is natural to start with a geometry wherein the $x = 0$ plane separates the N from the SF region:

$$\psi(x) = \psi(x) \theta(x) \quad (3)$$

with $\theta(x)$ the Heaviside function. This choice allows one to find the general solutions of the BdG Eqs. (1) in the N and SF phase. They read:

$$\begin{pmatrix} u_a^n \\ v_b^n \end{pmatrix} = \sum_{k_j} e^{ik_k x} r \begin{pmatrix} U_{k_j}^{p;n} e^{ik_p x} \\ V_{k_j}^{h;n} e^{ik_n x} \end{pmatrix}; \quad (4)$$

$$\begin{pmatrix} u_a^s \\ v_b^s \end{pmatrix} = \sum_{k_j} e^{ik_k x} r \left[\begin{pmatrix} U_{k_j}^{h;s} \\ V_{k_j}^{h;s} \end{pmatrix} e^{ik^h x} + \begin{pmatrix} U_{k_j}^{p;s} \\ V_{k_j}^{p;s} \end{pmatrix} e^{ik^p x} \right];$$

Here, the sub- and superscripts $n; s; p$ and h denote normal, superfluid, particle-like and hole-like respectively. We split the vectors k into their components parallel to the wall $k_x = (0; k_y; k_z)$ and the x -component k_p which relates to the $k_h^{p;h}$ by the BdG Eqs.:

$$k_h = \frac{k_p^2}{2m} - 4m(E + \hbar); \quad (5a)$$

$$k^{p;h} = \frac{k_p^2}{2m} + 2m\mu; \quad (5b)$$

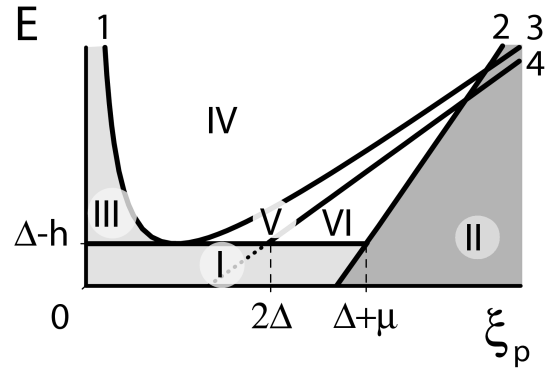


FIG. 2: The various scattering regions for an a -particle incident on the interface from the N side, as a function of its energy E and $k_p = k_p^2/2m$ (k_p is its momentum along the x -axis). The heavily-shaded region is energetically forbidden, while complete reflection occurs in the lightly-shaded regions. Particles in region VI may scatter to all states indicated in Fig. 1 by curly arrows. Above line 4 (regions IV and V), Andreev reflections do not occur, and above curve 3 (region IV), hole-like excitations are also impossible. The numbered curves are 1: $k_p = k_h^{p;h}$, 2: $k_p = k_a + E$, 3: $k_p = k_a + \mu$ and 4: $k_p = 2(E + \hbar)$.

where $k_h^{p;h} = E + \hbar \pm \frac{k_p^2}{2m}$. The amplitudes U and V from solutions (4) are determined by matching the wavefunctions and their derivatives at $x = 0$ [15]. Figure 1 shows the quasiparticle spectra in both the N region (left panel) and the SF region (right panel). In the former one recognizes two approximately linear energy branches a and b near the Fermi surfaces, while in the latter the spectra are gapped by \hbar and $\hbar + \mu$. Since we take $k_a > k_b$, the states belonging to the (lower) spectrum are the ones composed of a -particles and b -holes.

Scattering regimes — Consider an incoming a -particle from the N side with energy E and momentum k ; it is indicated in Fig. 1 by a curly arrow and its motion is completely characterized by E and $k_p = k^2/2m$. The crossover of either of the $k_h^{p;h}$ or k_k from real to imaginary (or vice versa) signifies a change in the scattering mechanism. The regions in the $E - k_p$ plane corresponding to the various such scattering processes are shown in Fig. 2; we now briefly describe them. If $E < \hbar$, the incoming particle has insufficient energy to excite quasiparticles inside the SF; it is completely reflected as a superposition of a particle and a hole. This region is labelled I in Fig. 2. The situation where $E < k_a$ is physically forbidden for obvious reasons; it is labelled II. Next, consider energies above the threshold \hbar . For $k_p < k_a$ (region III), the incoming particle can excite neither particle-like nor hole-like quasiparticles in the SF and must therefore undergo complete reflection, even though it appears to have sufficient energy for transmission. The situation is akin to that of a quantal particle incident on a potential step; if the angle of incidence exceeds a critical angle, the particle is reflected. Here, the critical angle is θ_c with

$\tan \theta_c = \frac{p}{(E + \hbar v_F)} = 1$, in which $\theta_c < \frac{\pi}{2}$ corresponds to $p < \hbar v_F$. For angles satisfying $\theta_c^+ < \theta_c^- < \frac{\pi}{2}$ (region IV), or $\theta_c^- < \theta_c^+ < \frac{\pi}{2}$, particle-like states may be excited in the SF, in contrast to hole-like states. When $p < 2(E + \hbar v_F)$ (regions IV and V), there are no reflected holes; that is, Andreev reflection does not occur. Thus, in region V, both particle-like and hole-like excitations are present in the SF, but Andreev reflection is impossible. Finally, in region VI, both particle-like and hole-like excitations, as well as Andreev and normal reflection are allowed. To summarize, the lightly-shaded regions in Fig. 2 describe a-particles which undergo complete reflection, while the rightmost, heavily-shaded region is unphysical. Only incoming particles in the unshaded regions may excite quasiparticles inside the SF. As for incoming holes, they are only transmitted in a region analogous to II in the diagram. Arguments very similar to the preceding, applied to incoming b-particles and a-holes (therefore the $\bar{\nu}$ -channel), lead to a diagram identical to that of Fig. 2 but with $\hbar v_F \rightarrow -\hbar v_F$.

The p - E diagrams of the deep BCS and the unitary regime have a different topology. In the deep BCS regime, the relation $2\mu_a + \mu_b$ implies that region VI of Fig. 2 is by far the most important. Quasiparticle reflections occur mostly via the Andreev mechanism which involves particle, but not energy, transport across the interface. In contrast, at unitarity where $2\mu_a > \mu_b$ (since $\mu_a \approx 1.6\mu_b$), regime VI does not even exist. This means that quasiparticles with energy above the threshold $\hbar v_F$ cannot undergo Andreev reflection but only normal (specular) reflection, in which neither particles nor energy are carried across the interface.

Thermal conductivity — In order to study the transport properties, we seek to relate the amplitudes U and V of Eqs. (4) to the transport coefficients, based on a conservation law for the current. From the BdG Eqs. it readily follows that the density $\rho(x) = j_a^\dagger j_a + j_b^\dagger j_b$ and the quasiparticle current

$$j = \frac{i}{2m} [u_a^\dagger r u_a - u_a r u_a^\dagger - v_b^\dagger r v_b + v_b r v_b^\dagger]$$

satisfy the continuity equation. The transmission coefficient $S(E; p)$ of an incoming particle of energy E and momentum k is defined as the ratio of the transmitted to the incoming current along the x -axis. S vanishes in regions I, II and III whereas for energies slightly above the transmission threshold $E = \hbar v_F$ (for regions V and VI),

$$S(E; p) \sim \frac{p}{E - \hbar v_F}; \quad (6)$$

similarly to the case of particles scattering from a Hartree potential of height $\hbar v_F$. Next, one can write the heat flux through the interface and to the $i = \pm$ branch as:

$$\bar{W}_{x,i} = \frac{m}{4} \int_{s=p/\hbar}^{\infty} d_s \int dE E f(E) S(E; s); \quad (7)$$

where $f(E)$ is the Fermi-Dirac distribution and the integration is performed over the p - E and $\hbar v_F$ - E planes (with

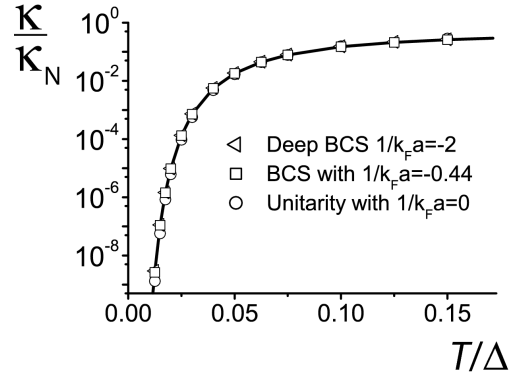


FIG. 3: The thermal conductivity across the N-SF interface divided by the normal-phase conductivity κ_N against $T = T_F \tau$ for the unitary, BCS and deep BCS cases. For $T \ll T_F$, κ/κ_N drops dramatically (notice the logarithmic scale). The curve represents the analytical result obtained by the use of the Andreev approximation, Eqn. (8). At unitarity, $\tau = 0.69T_F$, in the BCS case $\tau = 0.25T_F$ and in the deep BCS case $\tau = 0.002T_F$.

$\hbar v_F = k_F^2 = 2m$). In equilibrium, the N-SF flux is balanced by an equal SF-N flux. A small temperature bias on the N side will induce a net heat flow Q . By the Kapitza approach, the latter is $Q = T$ with the heat conductivity $\kappa = \kappa_N + \kappa_{SF}$.

We have analytically calculated the transmission coefficients for all regions of Fig. 2. To fix the values of $\hbar v_F$ and $T_F = k_F^2 = 2m = (3/2n)^2 = 2m$ for given $k_F a$ (n is the density in the SF), we have used the gap and number equations, as well as the exact $T = 0$ coexistence condition [13]. The resulting ratio of κ to the conductivity in the N phase, κ_N , is shown in Fig. 3 as a function of $T = T_F \tau$. We find that κ/κ_N decreases drastically below $T = 0.1$ [18]. Remarkably, κ/κ_N is almost independent of the interaction parameter $k_F a$. This can be understood as follows. For low enough temperature, $T \ll T_F$, only incident particles (and holes) with energies slightly above the threshold $E = \hbar v_F$ contribute to the heat conductivity because of their low statistical weight $f / e^{-(E - \hbar v_F)/T}$ appearing in eqn. (7). Furthermore, relation (6) shows that S displays the same behavior in regions V and VI. The main effect of varying $1/k_F a$ from large and negative (deep BCS) to zero (unitarity) is to move the boundary between regions V and VI to the right. Both the strong exponential decay with $\tau = T/T_F$ and the square root dependence of S on $E - \hbar v_F$ are unaffected by the variation of $1/k_F a$, hence the very similar behavior of κ/κ_N for all regimes under study.

These considerations are exemplified by the following calculation in the deep BCS regime, where the Andreev approximation may be used to obtain an analytical expression for κ . The approximation is to equate all the $k_{p,h}^{p,h}$ wave vectors and take the temperature to satisfy $T \ll T_F$.

We obtain

$$\chi_{BCS} = 2 \sum_{\mathbf{k}} \frac{P}{2m} \frac{e^{-(\epsilon_{\mathbf{k}} - \mu) = T} (\epsilon_{\mathbf{k}} - \mu)^2}{4 T^2}; \quad (8)$$

which amounts to Andreev's result when $\hbar = 0$ [1]. The summation denotes the excitations of the $(-)$ and $(+)$ states in the SF. The energy carried by the $(-)$ branch is a factor $e^{2\hbar = T}$ lower than that of the $(+)$ branch and due to coexistence $\hbar = T$, it can be neglected. Equation (8) demonstrates the exponential decay of χ_{BCS} with decreasing temperature. Although the Andreev approximation is invalid for the aforementioned experiments [4, 5], formula (8) as plotted in Fig. 3, provides a good estimate of χ_{BCS} , even beyond the BCS regime [19].

FFLO states — Andreev reflection may also produce effects similar to Fulde-Ferrell-Larkin-Ovchinnikov states (FFLO) as seen in Ref. 12. For the case of a SC, McMillan calculated [16] the first corrections to the gap function (3) due to self-consistency and found, at $T = 0$, a decaying oscillation of $\Delta(\mathbf{x})$ on the N side. This stems from the phase difference $(\mathbf{k}_p - \mathbf{k}_h)$ between the wavefunctions of incoming particles (holes) with momentum \mathbf{k}_p (\mathbf{k}_h) and energy E_p (E_h), and their Andreev reflected holes (particles) of momentum \mathbf{k}_h (\mathbf{k}_p); the wavefunctions of these determine the gap profile by $\Delta(\mathbf{x}) / \sum_{\mathbf{k}} u_{a,\mathbf{k}}(\mathbf{x}) v_{b,\mathbf{k}}(\mathbf{x})$. We speculate that this also happens beyond the BCS regime. In particular, the numerically observed $T = 0$ FFLO states for trapped gases at unitarity may be a consequence of the presence of the N-SF interface [12]. Note that the FFLO state is not thermodynamically stable for a homogeneous system at unitarity [9].

Discussion — In a SC, the heat conductivity also has a lattice component, which dominates the electronic component at low temperatures; the absence of such a component in the system under study makes the decrease of the conductivity more significant. Addition of the Hartree-Fock potentials amounts to a change of the coexistence condition (2) and a mere horizontal shift of lines 1 through 4 in Fig. 2, thereby preserving the energy gap (region I) and thus the main conclusions of our paper. We expect that improvements on our approximations, which are the use of the one-channel model, the gap profile (3), and the temperature dependence which is solely contained in the Fermi-Dirac function, will affect the results only quantitatively and mostly at unitarity. Finally, note that the values we used for \hbar ; μ and E_F are those at the interface. Estimating that T_F at unitarity (see caption of Fig. 3) is equal the reported T_F [4, 5], one concludes that the drop of conductivity sets in at $T = 0.05 T_F$, from which follows that our arguments indeed apply to the current experiments.

Conclusion — Scattering of quasiparticles off the N-SF interface, as summarized in Fig. 2, gives rise to the following effects. The thermal conductivity across the interface decreases rapidly with decreasing temperature at the experimentally realized temperatures, and is described by equation (8). This implies that thermalization slows down, and

a temperature difference across the interface can appear; the incorporation of this could lead recent models to better agreement with current experiments. We call for such incorporation, as well as for a separate temperature measurement of the N and SF phase since, as we have argued, they may not be the same. In addition, we argue that reflections of quasiparticles off the interface can induce modifications to (BCS regime), or even cause (at unitarity) gap oscillations, usually identified as FFLO state.

Acknowledgement — We acknowledge partial support by project FWO G.0115.06; AL and BVS is supported by GOA/2004/02; BVS is supported by IUAP P5/01. It is a pleasure to thank Henk Stoof and Koos Gubbels for discussions and useful suggestions and Joseph Indekeu for a careful reading of the manuscript.

-
- [1] A.F. Andreev, Zh. Eksp. Teor. Fiz. **46**, 1823 (1964) [Sov. Phys. JETP **19**, 1228 (1964)]; **49**, 655 (1966) [**22**, 455 (1966)].
 - [2] C.W.J. Beenakker, Rev. Mod. Phys. **69**, 731 (1997).
 - [3] G.E. Blonder, M. Tinkham, T.M. Klapwijk, Phys. Rev. B **25**, 4515 (1982).
 - [4] M.W. Zwierlein, C.H. Schunck, A. Schirotzek and W. Ketterle, Nature **442**, 54 (2006); Science **311**, 492 (2006).
 - [5] G.B. Partridge, W. Li, R.I. Kamar, Y.A. Liao and R.G. Hulet, Science **311**, 503 (2006); G.B. Partridge, W. Li, Y.A. Liao, R.G. Hulet, M. Haque and H.T.C. Stoof, Phys. Rev. Lett. **97**, 190407 (2006).
 - [6] K.B. Gubbels, M.W.J. Romans and H.T.C. Stoof, Phys. Rev. Lett. **97**, 210402 (2006); M. Haque and H.T.C. Stoof, Phys. Rev. A **74** 011602 (2006).
 - [7] T.N. De Silva and E.J. Mueller, Phys. Rev. Lett. **97**, 070402 (2006).
 - [8] F. Chevy, Phys. Rev. Lett. **96**, 130401 (2006).
 - [9] D.E. Sheehy and L. Radzihovsky, Phys. Rev. Lett. **96**, 060401 (2006); cond-mat/0607803.
 - [10] P.F. Bedaque, H. Caldas and G. Rupak, Phys. Rev. Lett. **91**, 247002 (2003); A. Imambekov, C.J. Bolech, M. Lukin and E. Demler, Phys. Rev. A **74**, 053626 (2006); Q. Chen, J. Stajic, S. Tan and K. Levin, Phys. Rep. **412**, 1 (2005).
 - [11] M.M. Parish, F.M. Marchetti, A. Lamacraft, B.D. Simons, cond-mat/0605744, Nature Phys. **3**, 124 (2007).
 - [12] P. Castorina, M. Grasso, M. Oertel, M. Urban and D. Zappalà, Phys. Rev. A **72**, 025601 (2005); J. Kinnunen, L.M. Jensen and P. Törmä, Phys. Rev. Lett. **96**, 110403 (2006); K. Machida, T. Mizushima and M. Ichioka, Phys. Rev. Lett. **97**, 120407 (2006).
 - [13] A. Lazarides and B. Van Schaeybroeck, in preparation.
 - [14] P.G. de Gennes, *Superconductivity of Metals and Alloys*, (Addison-Wesley, Reading, MA, 1989).
 - [15] J. Demers and A. Griffin, Can. J. Phys. **49**, 285 (1971).
 - [16] W.L. McMillan, Phys. Rev. **175**, 559 (1968).
 - [17] Strictly speaking, this is only valid if the trapping length is much longer than the interfacial length.
 - [18] The normal-state conductivity χ_N vanishes linearly with T .
 - [19] In the plot we include the next order term (in $T = \hbar$) in Eqn. (8).